DØnote 4542

Measurement of the WW production cross section in e^+e^-, $e^\pm\mu^\mp$ and $\mu^+\mu^-$ final states at DØ in Run II

The DØ Collaboration
URL: http://www-d0.fnal.gov

(Dated: August 3, 2004)

Data collected from April 2002 to March 2004 by the DØ experiment in Run II of the upgraded Fermilab Tevatron collider at a centre of mass energy of $\sqrt{s} = 1.96$ TeV have been used to measure the cross section of WW pair production in the e^+e^-, $e^\pm\mu^\mp$ and $\mu^+\mu^-$ final states. Data, corresponding to an integrated luminosity of 252 pb^{-1} in the e^+e^-, 235 pb^{-1} in the $e^\pm\mu^\mp$ and 224 pb^{-1} in the $\mu^+\mu^-$ final state have been analysed. Applying all selection criteria leaves six events in the e^+e^-, fifteen events in the $e^\pm\mu^\mp$ and four events in the $\mu^+\mu^-$ final state. The measured cross section is

$$\sigma_{p\bar{p}\to WW} = 13.8^{+4.3}_{-3.8}(\text{stat.})^{+1.0}_{-0.8}(\text{syst.}) \pm 0.9(\text{lum.})\text{pb} \ .$$

Preliminary Results for Summer 2004 Conferences

I. INTRODUCTION

The present note describes the measurement of the WW production cross section in e^+e^-, $e^\pm\mu^\mp$ and $\mu^+\mu^-$ final states in data collected by the DØ experiment at the Fermilab Tevatron collider at a centre of mass energy of $\sqrt{s} = 1.96$ TeV. The measurement of the WW cross section offers a good possibility to test the Standard Model (SM) prediction of $WW\gamma$ and WWZ couplings. Anomalous couplings or decays of new particles increase the WW production. It is assumed that the reader is familiar with the DØ detector [1].

WW pair production is a major background for searches of new particles, such as Higgs bosons with subsequent decay into WW pairs or associated Chargino and Neutralino production in the trilepton final states. Thus a good understanding of the WW production is desirable to optimise the selection criteria for the search of new particles.

The NLO prediction for the WW production cross section at a centre of mass energy of $\sqrt{s} = 2$ TeV is 13 pb using MRS98 and 13.5 pb for CTEQ5 parton distribution function [2]. The WW production cross section in $p\bar{p}$ collisions at a centre of mass energy of $\sqrt{s} = 1.8$ TeV is measured with a rather large error to be $\sigma_{p\bar{p}\to WW} = 10.2^{+6.3}_{-5.1}$(stat.)$\pm$1.6(syst.) pb [3].

Section II of this note describes the various data and MC samples used. Section III gives an overview of the event selection in the three different channels and shows some distributions of data and Monte Carlo comparisons. Section IV describes the different sources of systematic uncertainties. Section V provides a presentation of the cross section calculation.

II. DATA AND MONTE CARLO SAMPLES

This analysis uses data collected by the DØ experiment between April 2002 and March 2004 at the Fermilab Tevatron collider at a centre of mass energy of $\sqrt{s} = 1.96$ TeV. The total integrated luminosity analysed is in the range of $\int \mathcal{L}dt \approx 224 - 252\ pb^{-1}$ depending on the final state. All simulated events are generated using PYTHIA 6.202 [4] and ALPGEN [5] using the CTEQ5L parton distribution functions [6]. They are processed through a full detector simulation with an overlaid Poisson–distributed average of 0.8 minimum bias events. A top quark mass of $m_t = 175$ GeV/c^2 is used. Table I gives an overview of all Monte Carlo samples with their cross sections and references used in comparisons with data. The contribution from QCD events was estimated from data in a sample of like-sign di–lepton events with inverted lepton quality cuts.

The geometric and kinematic detection efficiencies for signal and background are determined using the PYTHIA Monte Carlo followed by a GEANT–based simulation of the DØ detector. All trigger and reconstruction efficiencies for electrons and muons are derived from the data.

III. EVENT SELECTION

A. ee-Selection

For the e^+e^- final state, events are selected based on single and di–electron triggers. Runs with failures of detector components are rejected. The total integrated luminosity for the di–electron sample is $\int \mathcal{L}dt = 252$ pb^{-1}. Events are

TABLE I: Cross sections times branching ratio for the various Monte Carlo samples and their references, used in comparisons with data. The cross sections are only given for a single lepton flavour. For decays with one electron and one muon in the final state, the cross section times branching ratio must be multiplied by a factor of two.

Process		$\sigma \times BR$ [pb]	Reference
$Z/\gamma^* \to \ell\ell$ $(\ell = e, \mu, \tau)$	15 GeV/c^2< $m_{\ell\ell}$< 60 GeV/c^2	465	[7]
	60 GeV/c^2< $m_{\ell\ell}$< 130 GeV/c^2	254	[7]
	130 GeV/c^2< $m_{\ell\ell}$< 250 GeV/c^2	2	[7]
$W \to \ell\nu$ inclusive $(\ell = e, \mu)$		2717	[7]
$WW \to \ell\nu\ell\nu$ $(\ell = e, \mu)$		0.147	[2]
$WZ \to \ell\nu\ell\ell$ $(\ell = e, \mu)$		0.014	[2]
$ZZ \to \ell\ell\ell\ell$ $(\ell = e, \mu)$		0.002	[2]
$t\bar{t} \to b\ell\nu b\ell\nu$ $(\ell = e, \mu)$		0.076	[8]
Υ(1s)$\to \ell\ell$		27	[4]
Υ(2s)$\to \ell\ell$		20	[4]

required to have two electrons satisfying standard electron identification criteria. The selection is based on isolation, electromagnetic fraction and shower shape criteria (HMatrix). Furthermore the electrons must pass a likelihood criterion of 0.3. Both electrons are required to come from the same vertex ($|\Delta z|$(tracks) < 2 cm) and should have opposite charge. The leading electron should have a transverse momentum of $p_T^{e_1} > 20$ GeV/c, the trailing electron should have a transverse momentum of $p_T^{e_2} > 15$ GeV/c (cut 1). The transverse momentum measurement of the electrons is based on calorimeter cell energy information.

The jet multiplicity in $Z/\gamma^* \to ee$ production is underestimated by the PYTHIA Monte Carlo. Since the kinematic distributions used in the analysis are expected to be sensitive to the number of jets, the $Z/\gamma^* \to ee$ Monte Carlo events are re-weighted to reproduce the jet multiplicity observed in data to correct this underestimation. The re-weighting factors for the e^+e^- channel are found to be 1.01, 1.07, 1.6 and 2.6 for 1, 2, 3 and 4 jets respectively. Events without any jets are scaled down by a factor of 0.995.

To reject the large contribution from Z/γ^* decays, a set of cuts is applied. The missing transverse energy is required to be $\not\!\!E_T > 30$ GeV (cut 2). The best significance for minimal transverse mass $\min(m_T^{e_1}, m_T^{e_2})$ measurement can be achieved with a cut of $\min(m_T^{e_1}, m_T^{e_2}) > 60$ GeV/c^2 (cut 3), where the transverse mass is given by $m_T = \sqrt{2p_T^{\ell}\not\!\!E_T(1-\cos\Delta\phi(\ell,\not\!\!E_T))}$. To remove remaining contributions from decays of the Z boson resonance, events with an invariant di–electron mass around the Z boson mass are rejected. Thus, only events that fulfil the condition $|m_{ee} - M_Z| > 15$ GeV/c^2 are taken further into account (cut 4).

Drell-Yan events, that pass the invariant mass cut, can be tested to see if the missing transverse energy is caused by a mis-measurement of jets in the event. For the calculation of the scaled missing transverse energy the energy fluctuation of the jet is projected to the transverse plane ($\sqrt{E_{jet}}\cdot\sin\theta_{jet}$). Using the opening angle between this projected energy fluctuation and the missing transverse energy ($\cos\Delta\phi\,(jet, \not\!\!E_T)$) provides a measure for the contribution of the jet to the missing transverse energy. Thus the scaled missing transverse energy is defined as

$$\not\!\!E_T^{\text{Scaled}} = \frac{\not\!\!E_T}{\sqrt{\sum_{jets}\left(\sqrt{E_{jet}}\cdot\sin\theta_{jet}\cdot|\cos\Delta\phi\,(jet,\not\!\!E_T)\,|\right)^2}}\,. \tag{1}$$

The scaled $\not\!\!E_T$ is required to be $\not\!\!E_T^{\text{Scaled}} > 15\ \sqrt{\text{GeV}}$ (cut 5).

To suppress contributions from $t\bar{t}$ events, the scalar sum of the transverse momenta of the jets H_T is not allowed to exceed 50 GeV/c (cut 6). Only jets passing standard jet identification criteria and with $p_T > 20$ GeV/c and $|\eta| < 2.5$ are considered. After this final selection, six events remain in the data. The main background contribution is from $W + jets/\gamma$ production. The left column of Table II summarises all selection criteria for the ee final state.

In Table III the predictions from the Monte Carlo are compared with the events observed in the data after every step of the selection. The signal efficiencies for the criteria described above were determined for the WW Monte Carlo. Starting from an efficiency of (28.2±0.3)% after initial ID and p_T selection in the e^+e^- final state, the major part of the efficiency is lost while trying to reject the huge $Z/\gamma^* \to ee$ background and the $W + jet/\gamma$ backgrounds that may lead to topologies similar to the WW signal. After the final selection criteria are applied the efficiency for the WW signal is (8.76±0.13)%. Taking an integrated luminosity of 252 pb^{-1} and assuming a cross section of 13 pb, 3.26±0.05 events are expected from WW production. The background estimate is 2.30±0.21.

Figure 1 shows the distribution of the transverse momentum for the leading (top left) and trailing electron (top right) after cut 1. The missing transverse energy $\not\!\!E_T$ (bottom left) is shown without applying a cut on $\not\!\!E_T$ and $\not\!\!E_T^{\text{scaled}}$ and the invariant mass m_{ee} (bottom right) is presented at the final selection without applying the mass criterion. Figure 2 shows the distribution of the scaled missing transverse energy (left) after the invariant mass criterion is applied (Cut 4) and the scalar sum of the jet transverse momenta after the cut on the scaled missing transverse energy (Cut 5) is applied (right).

B. $e\mu$-Selection

The events of the $e\mu$-selection must be triggered by an electron–muon trigger. Again runs with hardware failures are rejected resulting in a data sample corresponding to $\int \mathcal{L}dt = 235$ pb^{-1}. The events must have at least one electron matching the electron identification criteria and $p_T > 20$ GeV/c. Furthermore one muon satisfying loose muon identification criteria with $p_T > 15$ GeV/c is required. A muon is called "medium" if it has at least two hits in the inner layer wire chambers of the muon system and at least two hits in the wire chambers of the two outer layers. In addition, at least one hit in the inner and in the two outer scintillator layers of the muon system must be found. A "loose" muon is defined as a medium muon but allowing one of the medium muon tests to fail.

The muons must be matched to a central track. For muon tracks with no hits in the silicon tracker (SMT), the p_T of the muon is recalculated using the primary vertex as a constraint. To select isolated muons, a track isolation cut

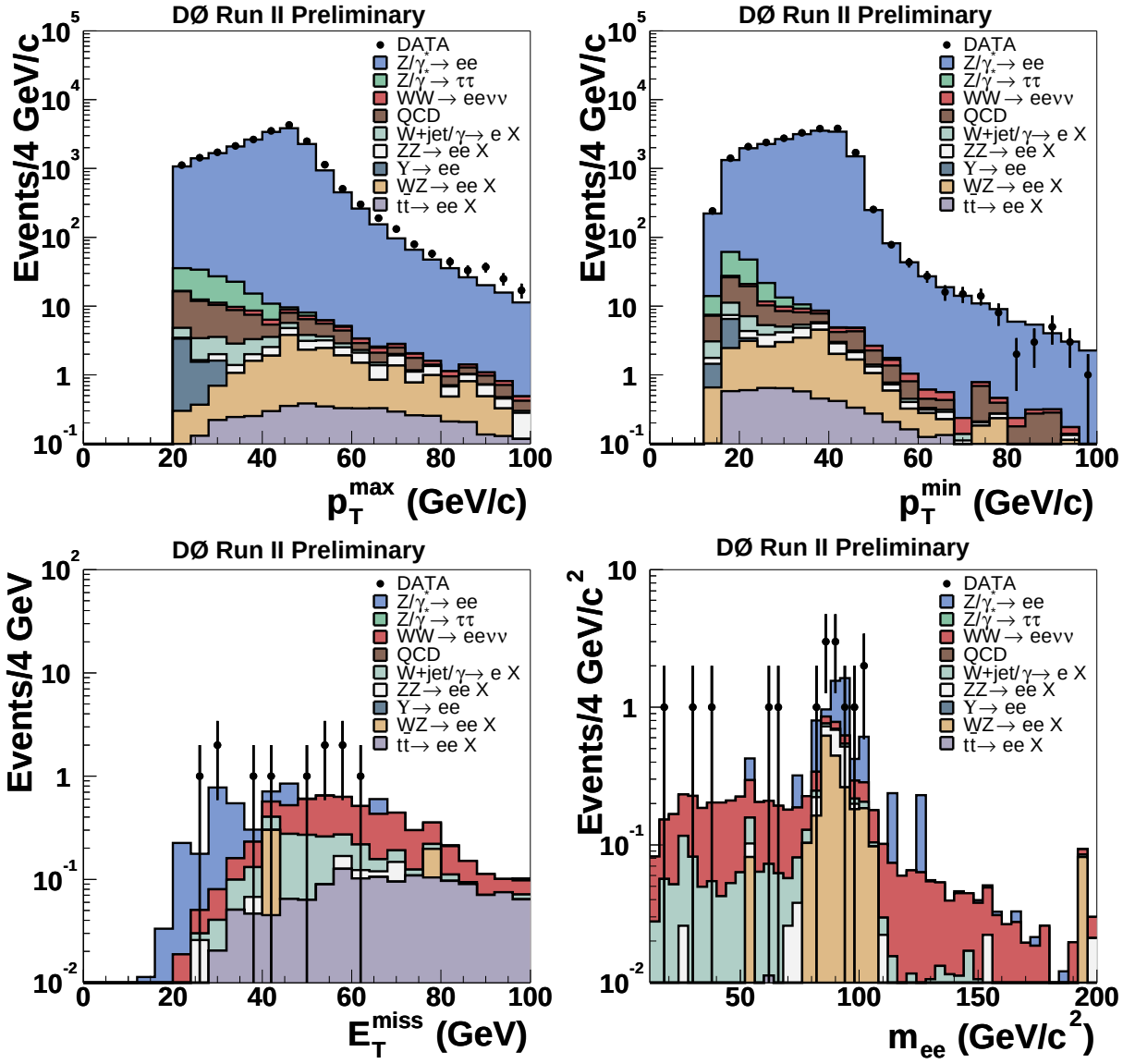

FIG. 1: Distribution for the e^+e^- channel of the transverse momentum for the leading (top left) and trailing electron (top right) for the ee channel after cut 1. The missing transverse energy $\not\!\!E_T$ (bottom left) is shown without applying the cut on $\not\!\!E_T$ and $\not\!\!E_T^{\rm scaled}$ and the invariant mass m_{ee} (bottom right) is shown after the final selection without applying the mass criterion. The Monte Carlo is normalised to the integrated luminosity in the data.

TABLE II: Summary of signal selection cuts for the ee, $e\mu$, and $\mu\mu$ channel.

	ee	$e\mu$	$\mu\mu$
Cut 1	$p_T^{e1} > 20\,\text{GeV}/c, p_T^{e2} > 15\,\text{GeV}/c$ opposite charge, $\lvert\Delta z\rvert$(tracks) < 2 cm	$p_T^e > 20$ GeV/c and $p_T^\mu > 15$ GeV/c opposite charge, $\lvert\Delta z\rvert$(tracks) < 2 cm $\lvert m_{ee} - M_Z\rvert > 30$ GeV/c^2 $\lvert m_{\mu\mu} - M_Z\rvert > 30$ GeV/c^2	$p_T^{\mu_1} > 20$ GeV/c and $p_T^{\mu_2} > 15$ GeV/c opposite charge
Cut 2	$\not\!\!E_T > 30\,\text{GeV}$	$\not\!\!E_T > 20\,\text{GeV}$	$\not\!\!E_T > 40\,\text{GeV}$
Cut 3	$\min(m_T^{e_1}, m_T^{e_2}) > 60$ GeV/c^2	$\min(m_T^e, m_T^\mu) > 20$ GeV/c^2	20 GeV/c^2 $< m_{\mu\mu} < 80$ GeV/c^2
Cut 4	$\lvert m_{ee} - M_Z\rvert > 15$ GeV/c^2	$H_T < 50$ GeV/c	$\chi^2_{\rm fit} > 20$
Cut 5	$\not\!\!E_T^{\rm Scaled} > 15\ \sqrt{\text{GeV}}$	$\not\!\!E_T^{\rm Scaled} > 15\ \sqrt{\text{GeV}}$	$\Delta\phi_{\mu\mu} < 2.4$
Cut 6	$H_T < 50$ GeV/c	$N^e_{SMT} \geq 3$ if 20 GeV/c^2 $< m_T^\mu < 110$ GeV/c^2	$H_T < 100$ GeV/c

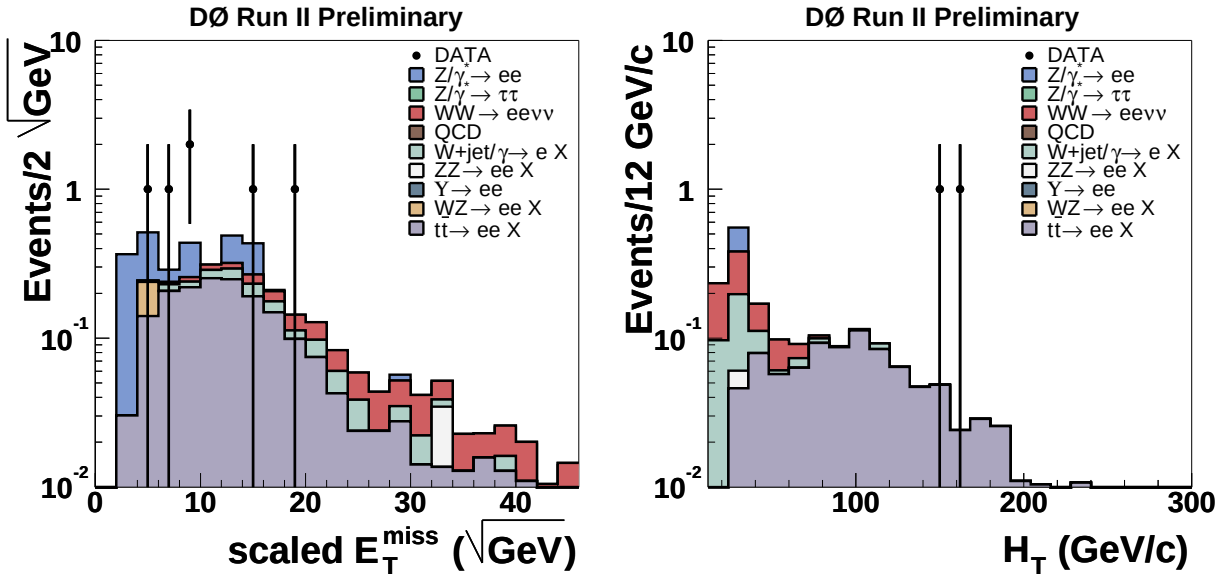

FIG. 2: Distribution for the e^+e^- channel of the scaled missing transverse energy after final selection without applying the cut on $\not\!\!E_T^{\rm scaled}$ and scalar sum of the jet transverse momenta after the cut on the scaled missing transverse energy (cut 5) is applied. Only events with at least one good reconstructed jet are shown.

TABLE III: Number of background and signal events expected, and number of events observed, after successive selections for an integrated luminosity of $\int \mathcal{L}dt = 252$ pb^{-1} in the e^+e^- channel. A cross section of 13 pb is assumed for the WW signal events. The statistical error is listed for all backgrounds. The error due to the uncertainty of the integrated luminosity is only given for the sum of all backgrounds.

	$t\bar{t}$	WZ	Υ	ZZ	$W+jet/\gamma$	$Z/\gamma^* \to \tau\tau$
Cut 1	5.72 ± 0.09	21.1 ± 1.4	5.15 ± 1.21	9.08 ± 0.42	11.6 ± 0.2	82.1 ± 4.1
Cut 2	4.98 ± 0.09	7.46 ± 0.80	0.00 ± 0.00	2.59 ± 0.22	8.07 ± 0.17	2.62 ± 0.60
Cut 3	2.60 ± 0.06	2.60 ± 0.47	0.00 ± 0.00	1.04 ± 0.14	1.70 ± 0.08	0.0 ± 0.0
Cut 4	2.08 ± 0.06	0.33 ± 0.17	0.00 ± 0.00	0.21 ± 0.06	1.42 ± 0.07	0.0 ± 0.0
Cut 5	0.89 ± 0.04	0.33 ± 0.17	0.00 ± 0.00	0.19 ± 0.06	1.27 ± 0.07	0.0 ± 0.0
Cut 6	0.18 ± 0.02	0.33 ± 0.17	0.00 ± 0.00	0.19 ± 0.06	1.25 ± 0.07	0.0 ± 0.0

	$Z/\gamma^* \to ee$	QCD	Background sum	WW signal	Data
Cut 1	20348 ± 46	51.2 ± 2.5	20534 ± 46 ± 1335	10.4 ± 0.1	21901
Cut 2	146 ± 4	3.24 ± 0.62	175 ± 4 ± 11	7.12 ± 0.07	181
Cut 3	11.8 ± 1.1	0.00 ± 0.00	20.0 ± 1.2 ± 1.3	4.14 ± 0.05	26
Cut 4	1.54 ± 0.14	0.00 ± 0.00	5.76 ± 0.25 ± 0.27	3.41 ± 0.05	12
Cut 5	0.28 ± 0.08	0.00 ± 0.00	3.15 ± 0.21 ± 0.20	3.31 ± 0.05	8
Cut 6	0.20 ± 0.06	0.00 ± 0.00	2.30 ± 0.21 ± 0.15	3.26 ± 0.05	6

is applied. The scalar sum of the transverse momenta of all tracks in a cone of $\Delta\mathcal{R} < 0.5$ around the muon track must be less than 4 GeV/c. To reject cosmic muons a scintillator timing cut in the muon system and the distance of closest approach of the track with respect to the primary vertex in the rz–plane ($d0^{\mu}_{\rm Vtx}$) and in the xy–plane ($z0^{\mu}_{\rm Vtx}$)

$$(d0^{\mu}_{\rm Vtx}/0.16\,{\rm cm})^2 + (z0^{\mu}_{\rm Vtx}/0.5\,{\rm cm})^2 < 1 \qquad (2)$$

is used. Both leptons should come from the same vertex ($|\Delta z|$(tracks) < 2 cm) and are required to have opposite charge. Furthermore events are rejected if a third lepton is found and the invariant mass of leptons of the same flavour is in the mass range from 60 to 120 GeV/c^2 (cut 1, Table II). This leaves 205 events in the data.

After the implementation of the lepton identification and kinematic criteria, the dominant background in the selected sample is from $Z/\gamma^* \to \tau\tau$ decays. Other background sources are $W + jet/\gamma$ events, where either the jet fakes an electron or isolated muon or the W boson radiates a photon that converts into an electron–positron pair,

TABLE IV: Number of background and signal events expected, and number of events observed, after successive selections for an integrated luminosity of $\int \mathcal{L}dt = 235$ pb^{-1} in the $e^{\pm}\mu^{\mp}$ channel. A cross section of 13 pb is assumed for the WW signal events. The statistical error is listed for all backgrounds. The error due to the uncertainty of the integrated luminosity is only given for the sum of all backgrounds.

	$t\bar{t}$	WZ	ZZ	$W + jet/\gamma$	$Z/\gamma^* \to \tau\tau$
Cut 1	7.84 ± 0.15	0.57 ± 0.02	0.13 ± 0.05	7.89 ± 0.16	143 ± 5
Cut 2	7.41 ± 0.14	0.50 ± 0.02	0.09 ± 0.04	6.15 ± 0.14	25.5 ± 2.1
Cut 3	6.24 ± 0.13	0.44 ± 0.02	0.07 ± 0.04	5.46 ± 0.13	3.47 ± 0.82
Cut 4	0.46 ± 0.04	0.41 ± 0.02	0.04 ± 0.03	5.13 ± 0.13	1.67 ± 0.56
Cut 5	0.35 ± 0.03	0.39 ± 0.02	0.04 ± 0.03	4.72 ± 0.12	0.0 ± 0.10
Cut 6	0.34 ± 0.03	0.38 ± 0.02	0.02 ± 0.02	2.72 ± 0.07	0.0 ± 0.10

	$Z/\gamma^* \to \mu\mu$	QCD	Background sum	WW signal	Data
Cut 1	13.5 ± 0.4	13.8 ± 1.1	187 ± 5 ± 12	15.6 ± 0.2	205
Cut 2	6.37 ± 0.32	5.95 ± 0.55	52.0 ± 2.2 ± 3.4	12.8 ± 0.1	66
Cut 3	0.70 ± 0.11	1.61 ± 0.35	18.0 ± 0.9 ± 1.2	11.9 ± 0.1	35
Cut 4	0.42 ± 0.09	0.42 ± 0.17	8.55 ± 0.61 ± 0.56	11.6 ± 0.1	22
Cut 5	0.37 ± 0.09	0.07 ± 0.07	5.94 ± 0.20 ± 0.39	11.1 ± 0.1	18
Cut 6	0.28 ± 0.09	0.07 ± 0.07	3.81 ± 0.17 ± 0.25	10.8 ± 0.1	15

and multi–jet production. No significant $\not\!\!E_T$ is expected from the latter. Remaining contributions from $Z/\gamma^* \to \mu\mu$ decays and also a fraction of the $Z/\gamma^* \to \tau\tau$ events can be rejected by requiring $\not\!\!E_T > 20$ GeV (cut 2).

The minimal transverse mass $\min(m_T^e, m_T^\mu)$ is expected to peak at small values for $Z/\gamma^* \to \tau\tau$ decays. Thus the minimal transverse mass is required to be $\min(m_T^e, m_T^\mu) > 20$ GeV/c^2 (cut 3). After this selection, 35 events remain in the data. The main background contribution after these cuts are $t\bar{t}$ decays, which (together with multi-jet events from QCD production) can be suppressed with an H_T criterion. Requiring $H_T < 50$ GeV/c (cut 4) rejects a large fraction of these events without decreasing the signal efficiency significantly. To reduce the Z/γ^* contribution a cut on the scaled missing transverse energy is applied: $\not\!\!E_T^{\text{Scaled}} > 15\ \sqrt{\text{GeV}}$ (cut 5).

$W + \gamma$ events with the γ converting into an electron positron pair can be rejected by requiring at least three hits in the silicon tracker for the electron track. This criterion is only applied if the transverse mass computed from muon, electron and $\not\!\!E_T$ is consistent with the W transverse mass and the primary vertex is in the acceptance of the silicon tracker (cut 6). After this final selection 15 events remain in the data. A summary of the selection criteria can be found in Table II.

Table IV gives an overview on the number of expected and observed events for every step of the selection. In the $e^{\pm}\mu^{\mp}$ final state, the event preselection efficiency for the WW signal at the beginning is (22.3±0.2)%. At the end of the selection, the WW efficiency is (15.4±0.2)%. Using again a cross section of 13 pb and an integrated luminosity of 235 pb^{-1}, the expected number of events from WW decays is 10.8±0.1. The predicted background is 3.8±0.2 events, and is dominated by the $W + jet/\gamma$ production. Figure 3 shows the distribution the transverse momentum of the leading (top left) and trailing lepton (top right) after the preselection (cut 1), the missing transverse energy $\not\!\!E_T$ (bottom left) after final selection without applying the $\not\!\!E_T$ criterion and minimal transverse mass (bottom right) after final selection without applying the transverse mass criterion. Figure 4 shows the distribution of the sum of jet momenta H_T at the end of the selection without applying the H_T criterion (left) and distribution of the scaled missing transverse energy $\not\!\!E_T^{\text{Scaled}}$ at the end of the selection without applying the $\not\!\!E_T^{\text{Scaled}}$ criterion (right).

C. $\mu\mu$-Selection

Events that pass the $\mu\mu$ selection should be triggered by one of four di–muon triggers or a single muon trigger that each have muon requirements at the trigger level 1 and 2. Three triggers have additional track requirements at the trigger level 3. The luminosity of this sample is $\int \mathcal{L}dt = 224\,\text{pb}^{-1}$. Events are required to have two muons of "loose" quality matched to a corresponding central track. To reject cosmics a cut on the scintillator times in the muon system is made. The transverse momentum of central tracks that have no hits in the silicon tracker is recalculated by constraining these tracks to the measured vertex of the event. All selected muon tracks are required to originate from the vertex region by a cut on the distance of closest approach of the tracks to the primary vertex as in Equation 2. All selected muons should fulfil the tracking isolation criterion $\sum_{\text{tracks}}^{\mathcal{R}<0.5} p_T < 4.0$ GeV/c. The transverse momentum

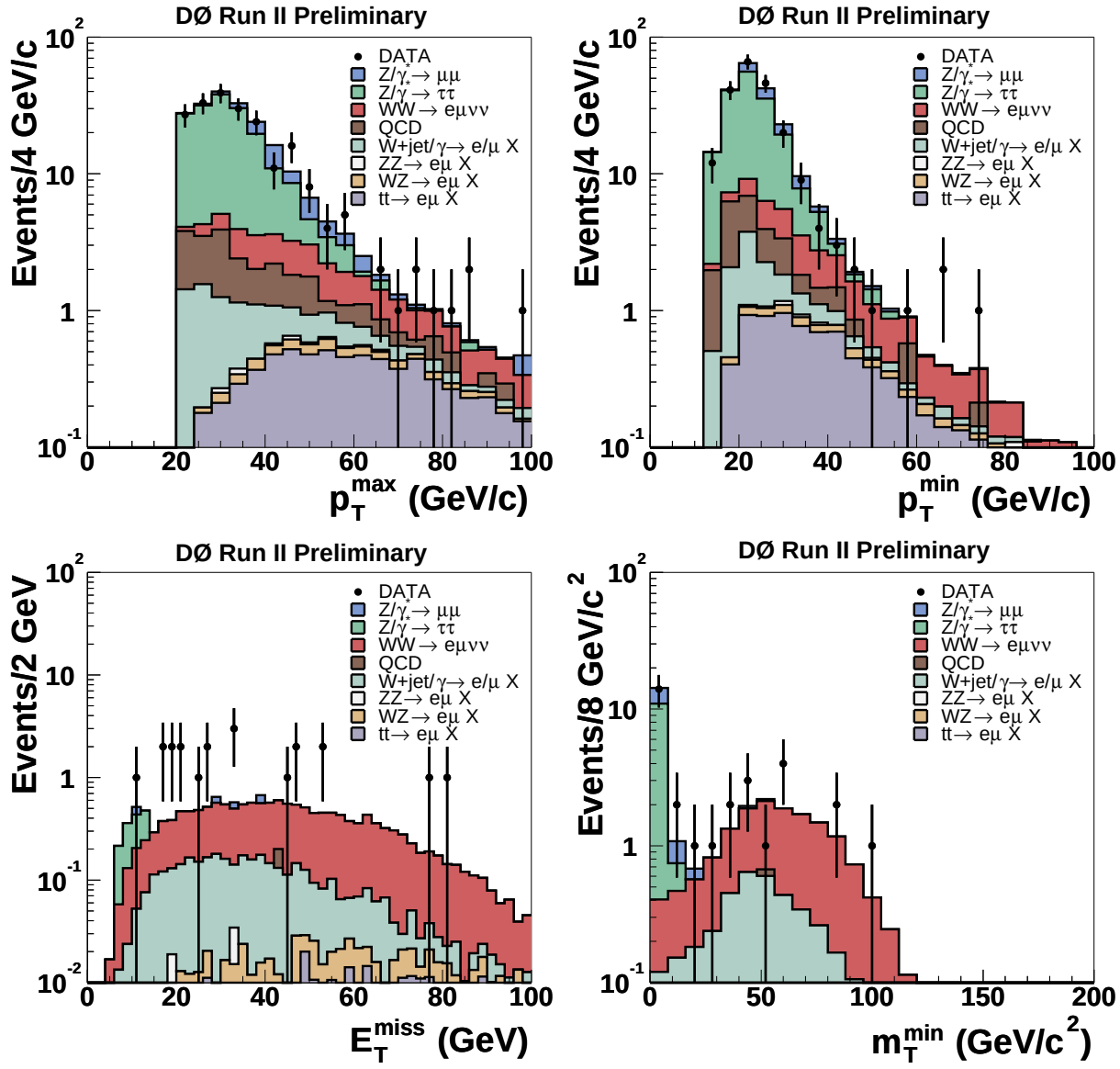

FIG. 3: Distributions for the $e^{\pm}\mu^{\mp}$ channel of the transverse momentum of the leading (top left) and trailing lepton (top right) after the preselection (cut 1) and the missing transverse energy $\not\!\!E_T$ (bottom left) after final selection withuot applying the $\not\!\!E_T$ criterion and minimal transverse mass (bottom right) after final selection without applying the minimal transverse mass criterion. The Monte Carlo is normalised to the integrated luminosity in the data.

of the leading muon should be $p_T^{\mu_1} > 20$ GeV/c, whereas the trailing muon should have $p_T^{\mu_2} > 15$ GeV/c.

To suppress backgrounds with similar event topologies as WW production a set of cuts is applied as follows: To account for the neutrinos in the WW production and to suppress background from Z/γ^* production, the missing transverse energy is required to be $\not\!\!E_T > 40$ GeV (cut 2). Events are required to have a di–muon invariant mass in the range of 20 GeV/c^2 $< m_{\mu\mu} <$ 80 GeV/c^2 (cut 3). The lower cut rejects events from J/ψ and Υ production, whereas the higher cut rejects events from Z/γ^* production. Since the momentum resolution is decreasing for tracks with high transverse momentum an additional constrained fit of all events is performed testing if these events are compatible with Z boson production. This fit uses a χ^2 minimisation with a Z boson mass constraint and $p_T^{\mu_1}$ as variation parameter for MINUIT:

$$\chi^2_{\rm fit} = \left(\frac{1/p_T^{\mu_1} - 1/p_T^{\mu_1,fit}}{1/\Delta p_T^{\mu_1}}\right)^2 + \left(\frac{1/p_T^{\mu_2} - 1/p_T^{\mu_2,fit}}{1/\Delta p_T^{\mu_2}}\right)^2 + \left(\frac{\vec{p}_T^{\,Had} + \vec{p}_T^{\,\mu_1,fit} + \vec{p}_T^{\,\mu_2,fit}}{\Delta p_T^{Had+\mu_1+\mu_2}}\right)^2 \quad (3)$$

The hadronic recoil is calculated from the missing transverse momentum $\not\!\!E_T$ in the event and all errors are derived

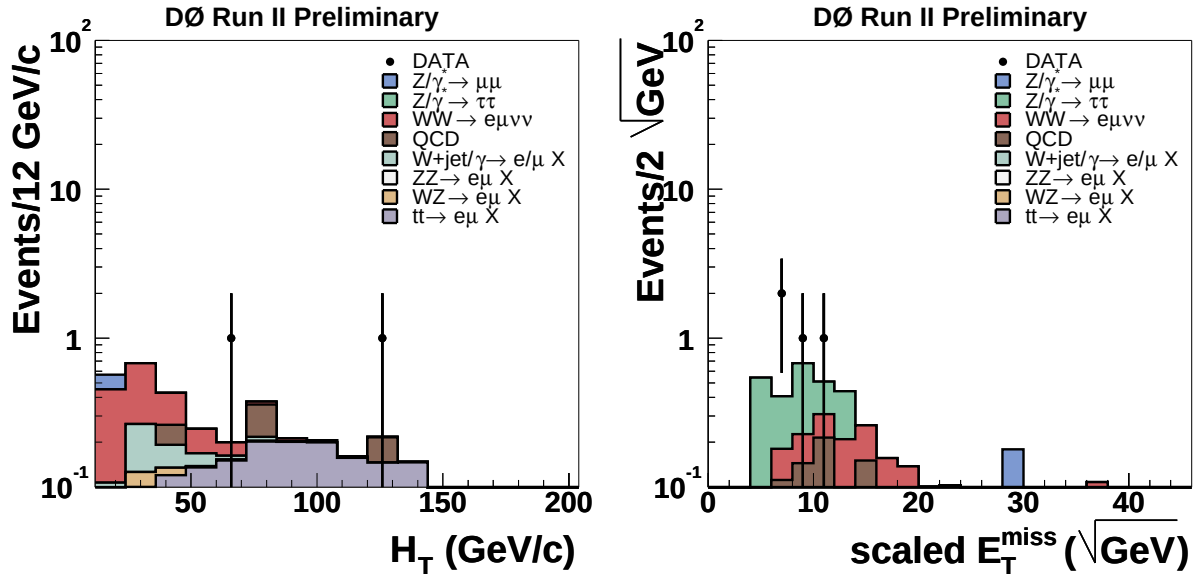

FIG. 4: Distribution for the $e^{\pm}\mu^{\mp}$ channel of the sum of jet momenta H_T at the end of the selection without applying the H_T criterion (left) and distribution of the scaled missing transverse energy $\not\!\!E_T^{\rm Scaled}$ at the end of the selection without applying the $\not\!\!E_T^{\rm Scaled}$ criterion (right). Only events with at least one good reconstructed jet are shown.

from a parametrisation of the Monte Carlo corresponding to the data resolution. The best signal efficiency over background rejection is achieved by a cut on $\chi^2 > 20$ (cut 4). To further suppress background from Z/γ^* production a cut on the opening angle of the muons in the azimuthal plane is introduced by $\Delta\phi_{\mu\mu} < 2.4$ (cut 5). To reject events from multi–jet, namely $t\bar{t}$ production, the scalar sum H_T of the transverse energy of all good jets is required to be $H_T < 100$ GeV (cut 6). The right column of Table II summarises the selection in the $\mu^+\mu^-$ channel.

Table V gives an overview on the number of expected and observed events for every step of the selection. After this final selection, four events remain in the data. For the $\mu^+\mu^-$ channel, the efficiency for WW production at the beginning of the selection is (31.5±0.2)%. Applying all the different selection criteria reduces the efficiency to (6.22±0.15)%. The expected number of WW events is 2.01±0.05 assuming the cross section of 13 pb and an integrated luminosity of 224 pb^{-1}. The expectations from all the backgrounds is 1.94±0.41 events. The $Z/\gamma^* \to \mu\mu$ decays contribute more than two thirds to this background expectation.

Figure 5 shows the distribution of the invariant di–muon mass (top left), missing transverse energy $\not\!\!E_T$ (top right) and the muon transverse momentum p_T (bottom left) for data and Monte Carlo after cut 1. The sum of jet transverse momenta is shown for events with at least one good reconstructed jet after cut 4 (Fig. 5 bottom right).

Figure 6 shows the distribution the invariant di–muon mass $m_{\mu\mu}$ (left) and the muon azimuthal opening angle $\Delta\phi_{\mu\mu}$ after all cuts (right).

IV. SYSTEMATIC STUDIES

Various sources of systematic uncertainties have been studied to investigate their influence on the WW cross section measurement in the various channels.

- The jet energy scale was varied by $\pm 1\sigma$.
- The influence of the electron and muon momentum smearing was tested by changing the smearing and calibration parameters by $\pm 1\sigma$.
- The branching ratio of the W boson into electrons and muons also affects the cross section measurement. Thus it was varied within its experimental errors by $\pm 1\sigma$ [9].
- The Z/γ^* cross section is varied within the theoretical uncertainty of ±3.6%.
- The $t\bar{t}$ cross section is varied by +5.9% and −14.7% [8].

TABLE V: Number of background and signal events expected, and number of events observed, after successive selections for an integrated luminosity of $\int \mathcal{L}dt = 224$ pb^{-1} in the $\mu^+\mu^-$ channel. A cross section of 13 pb is assumed for the WW signal events. The statistical error is listed for all backgrounds. The error due to the uncertainty of the integrated luminosity is only given for the sum of all backgrounds.

	$Z/\gamma^* \to \mu\mu$	QCD/W + jet	$Z/\gamma^* \to \tau\tau$	WZ	ZZ
Cut 1	17656 ± 41	5.6 ± 0.6	83.4 ± 3.7	8.8 ± 0.6	7.6 ± 0.4
Cut 2	410.8 ± 5.8	1.4 ± 0.3	1.0 ± 0.4	2.6 ± 0.3	1.5 ± 0.2
Cut 3	40.8 ± 1.8	0.8 ± 0.2	0.3 ± 0.2	0.6 ± 0.2	0.25 ± 0.07
Cut 4	9.6 ± 0.8	0.6 ± 0.2	0.03 ± 0.03	0.19 ± 0.09	0.10 ± 0.04
Cut 5	3.0 ± 0.5	0.2 ± 0.1	0.0 ± 0.0	0.15 ± 0.08	0.10 ± 0.04
Cut 6	1.6 ± 0.4	0.01 ± 0.01	0.0 ± 0.0	0.15 ± 0.08	0.10 ± 0.04

	$t\bar{t}$	Background sum	WW signal	Data
Cut 1	4.74 ± 0.04	17766 ± 40 ± 1155	10.1 ± 0.1	17770
Cut 2	3.46 ± 0.03	420.7 ± 5.8 ± 27.4	5.20 ± 0.08	448
Cut 3	1.59 ± 0.02	44.2 ± 1.9 ± 2.9	2.80 ± 0.06	55
Cut 4	1.02 ± 0.02	11.6 ± 0.8 ± 0.8	2.10 ± 0.05	17
Cut 5	0.91 ± 0.02	4.36 ± 0.52 ± 0.28	2.03 ± 0.05	5
Cut 6	0.09 ± 0.01	1.94 ± 0.41 ± 0.13	2.01 ± 0.05	4

TABLE VI: Summary of the systematic uncertainties of the WW production cross section among the three channels.

	Change of the WW cross section					
	e^+e^-		$e^\pm\mu^\mp$		$\mu^-\mu^+$	
Jet energy scale	+3.2%	−3.2%	+1.6%	−1.2%	+7.2%	−4.8%
Muon smearing	−	−	+4.7%	−2.2%	+10.0%	−4.1%
Electron smearing	+4.6%	−2.9%	+1.3%	−1.1%	−	−
BR($W \to \ell\nu$)	+4.4%	−3.9%	+5.3%	−4.6%	+4.3%	−4.1%
$\sigma(Z/\gamma^*, t\bar{t})$	+0.9%	−0.7%	+0.4%	−0.4%	+3.2%	−3.2%
$W + jets$	+4.0%	−4.0%	+3.0%	−3.0%	−	−
Jet re-weighting	+4.3%	−4.4%	−	−	+1.5%	−1.5%
Total	+9.2%	−8.3%	+8.0%	−6.2%	+13.5%	−8.3%

- The variation of the $W + jet$ background was varied within its uncertainty of ±12%.
- The systematic error caused by the re-weighting due to the underestimation of jet multiplicities by PYTHIA is determined.

Table VI summarises the systematic uncertainties of the WW production cross section among the three channels.

V. MEASUREMENT OF THE CROSS SECTION

The cross section is estimated separately for all three final states before combining it. To estimate the cross section, the likelihood method described in [10, 11] is used. Poissonian statistics are used to take into account the small number of events. The cross section σ is given by the equation

$$\sigma = \frac{n - N_{bg}}{\int \mathcal{L}dt \cdot BR \cdot \epsilon} \ , \tag{4}$$

where n is the number of observed events, N_{bg} the expected background contribution. $\int \mathcal{L}dt$ is the integrated luminosity, BR the branching fraction and ϵ the efficiency for the signal. The likelihood for n events in the data is given by

$$L(\sigma, n, N_{bg}, \int \mathcal{L}dt, BR, \epsilon) = \frac{\tilde{N}^n}{n!} e^{-\tilde{N}} \ , \tag{5}$$

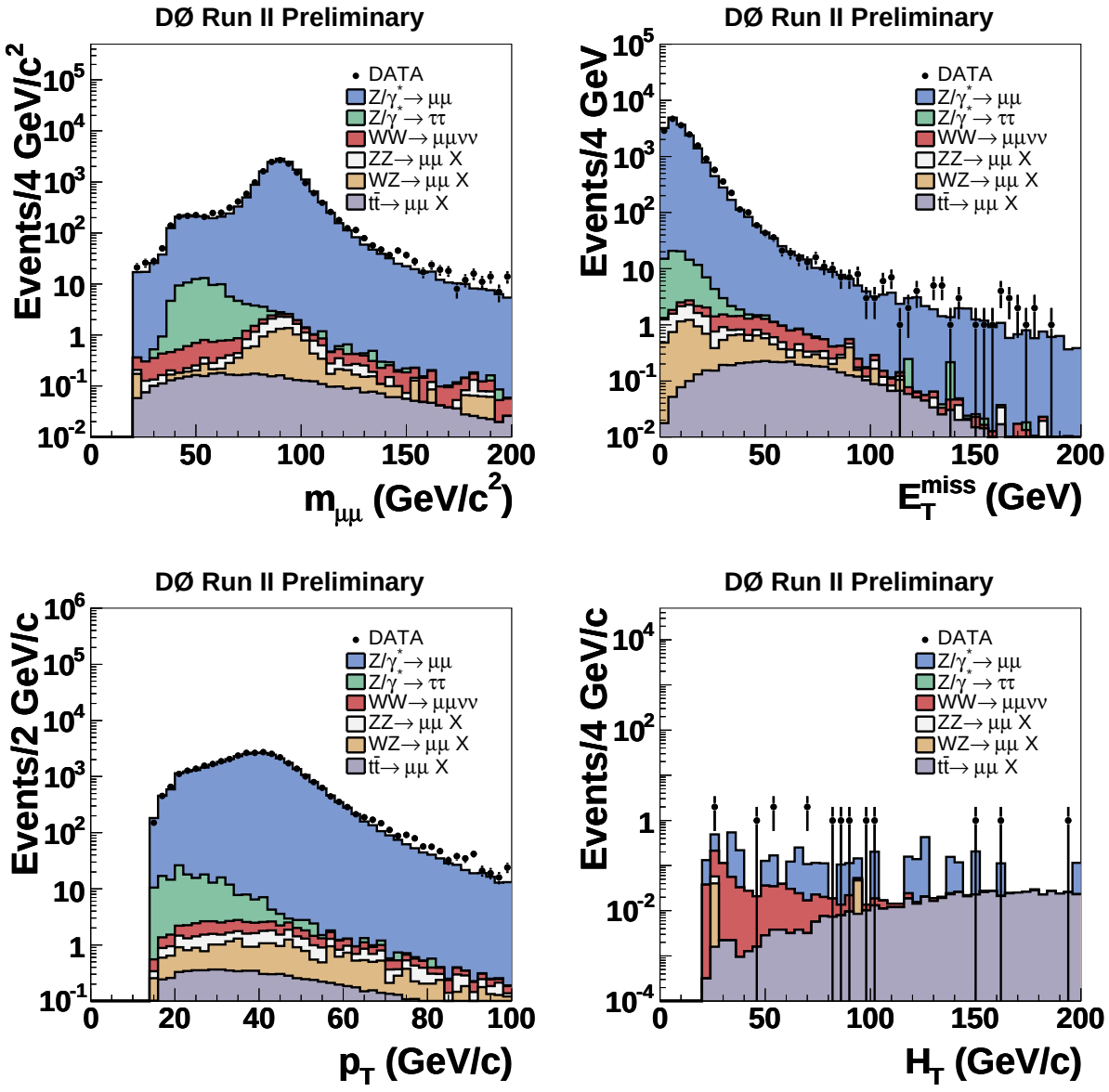

FIG. 5: Distributions for the $\mu^+\mu^-$ channel of the di–muon invariant mass $m_{\mu\mu}$ (top left), missing transverse energy $\not\!\!E_T$ (top right), the muon transverse momentum p_T (bottom left) for data and Monte Carlo after cut 1. The sum of jet transverse momenta (bottom right) is shown for events with at least one good reconstructed jet after cut 4. The Monte Carlo is normalised to the integrated luminosity in the data.

where $\tilde{N}$ is the number of signal and background events:

$$\tilde{N} = \sigma \cdot BR \cdot \int \mathcal{L}dt \cdot \epsilon + N_{bg} \ . \tag{6}$$

The cross section σ can be estimated by minimising $-2\ln L(\sigma, n, N_{bg}, \int \mathcal{L}dt, BR, \epsilon)$. To combine the channels the likelihood functions can simply be multiplied:

$$L_{comb}(\sigma, n, N_{bg}, \int \mathcal{L}dt, BR, \epsilon) = \prod_{i=1}^{N_{channel}} \frac{\tilde{N}_i^{n_i}}{n_i!} e^{-\tilde{N}_i} \ . \tag{7}$$

For the di–electron final state, the measurement yields a cross section of

$$\sigma(p\bar{p} \to WW) = 14.59^{+11.01}_{-8.39}(\text{stat.})^{+1.34}_{-1.21}(\text{syst.}) \pm 0.95(\text{lum.})\text{pb} \ . \tag{8}$$

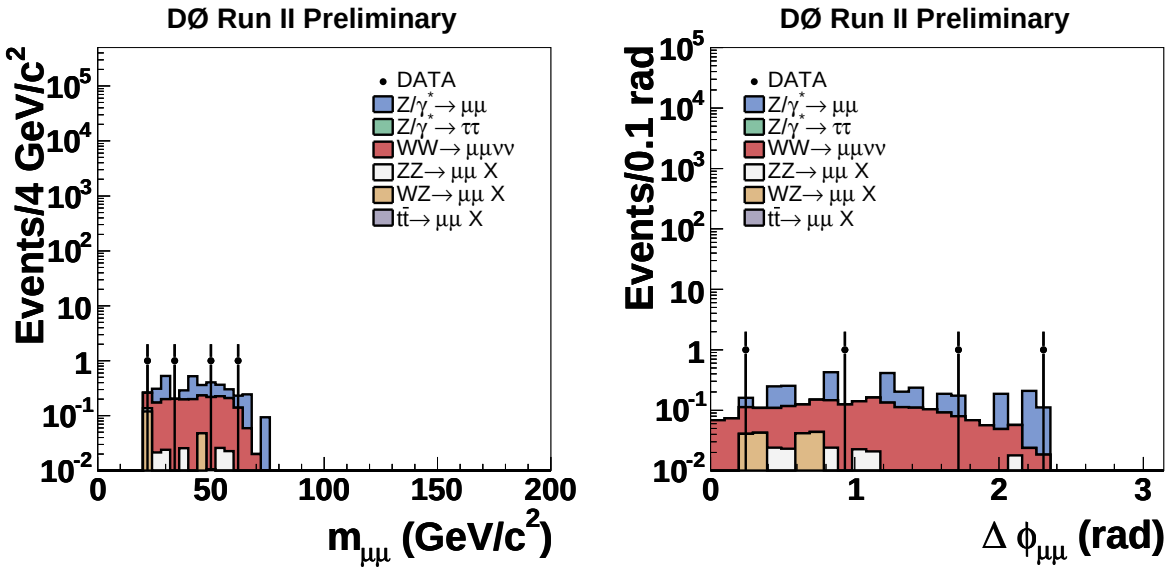

FIG. 6: Distribution of the invariant di–muon mass $m_{\mu\mu}$ (left) and the muon azimuthal opening angle $\Delta\phi_{\mu\mu}$ after all cuts (right) for the $\mu^+\mu^-$ channel.

The measurement in the $e^{\pm}\mu^{\mp}$ final state yields a cross sections of

$$\sigma(p\bar{p} \rightarrow WW) = 13.64^{+5.14}_{-4.32}(\text{stat.})^{+1.09}_{-0.85}(\text{syst.}) \pm 0.89(\text{lum.})\text{pb} \ . \tag{9}$$

For the $\mu^+\mu^-$ final state, the measurement yields a cross sections of

$$\sigma(p\bar{p} \rightarrow WW) = 13.22^{+14.78}_{-10.72}(\text{stat.})^{+1.78}_{-1.10}(\text{syst.}) \pm 0.86(\text{lum.})\text{pb} \ . \tag{10}$$

The combined result of the cross section measurement is

$$\sigma(p\bar{p} \rightarrow WW) = 13.77^{+4.31}_{-3.76}(\text{stat.})^{+0.96}_{-0.81}(\text{syst.}) \pm 0.90(\text{lum.})\text{pb} \ . \tag{11}$$

Figure 7 (left) presents the likelihood distribution for the combined measurement. For the combination of the systematic errors, the full correlation between the individual errors and channels is taken into account.

The significance of the signal observation can be obtained with a likelihood ratio method [12]. The confidence level distributions CL_b and CL_{s+b} for $6 \cdot 10^7$ toy Monte Carlo experiments are shown in Fig. 7 (right). CL_b and CL_{s+b} are defined as

$$CL_b = P(Q \leq Q_{obs}|background) \text{ and } CL_{s+b} = P(Q \leq Q_{obs}|signal + background) \tag{12}$$

where the test statistics Q is given by

$$Q = \frac{P_{Poisson}(data|signal + background)}{P_{Poisson}(data|background)} = \frac{\prod_{nch} \frac{(s_i+b_i)^{n_i} e^{-(s_i+b_i)}}{n_i!}}{\prod_{nch} \frac{(b_i)^{n_i} e^{-b_i}}{n_i!}} \ . \tag{13}$$

For the combined measurement, the significance is found to be $\sigma = 5.2$.

VI. CONCLUSIONS

A first measurement of the WW production cross section with DØ data recorded between April 2002 and March 2004 at a centre of mass energy of $\sqrt{s} = 1.96$ TeV has been performed using di–electron, electron–muon and di–muon final states. The combined results yield a cross section of

$$\sigma(p\bar{p} \rightarrow WW) = 13.8^{+4.3}_{-3.8}(\text{stat.})^{+1.0}_{-0.8}(\text{syst.}) \pm 0.9(\text{lum.})\text{pb} \ . \tag{14}$$

which is in good agreement with the prediction from next-to-leading order calculations. Using the likelihood ratio method a significance of 5.2σ is found for WW production.

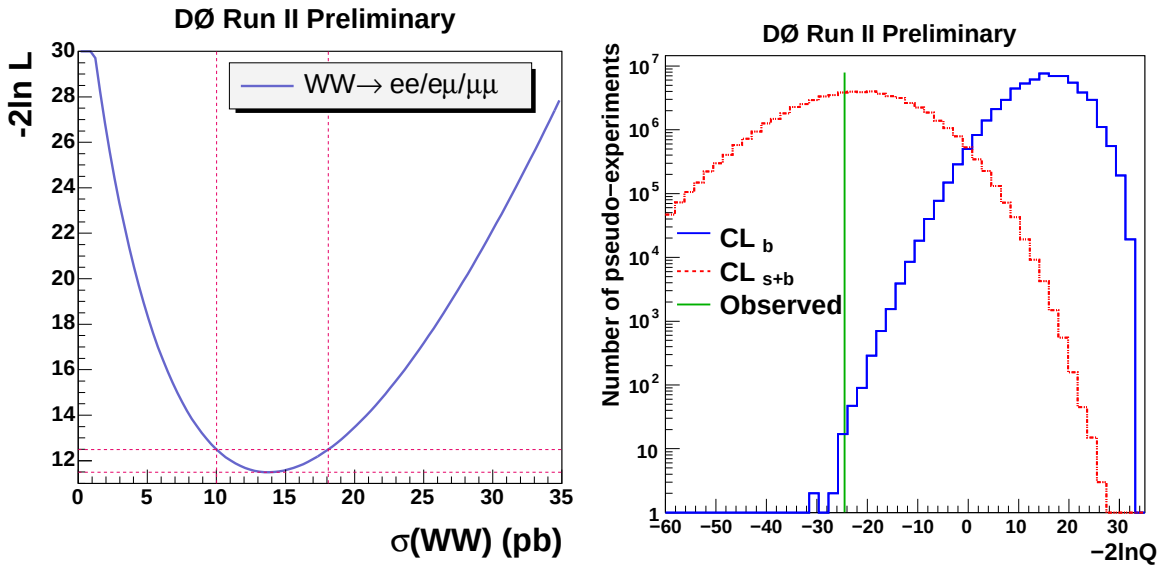

FIG. 7: Likelihood distributions for the the combination of all channels (left) and CL_b and CL_{s+b} distributions for $6 \cdot 10^7$ toy Monte Carlo experiments (right).

Acknowledgments

We thank the staffs at Fermilab and collaborating institutions, and acknowledge support from the Department of Energy and National Science Foundation (USA), Commissariat à l'Energie Atomique and CNRS/Institut National de Physique Nucléaire et de Physique des Particules (France), Ministry of Education and Science, Agency for Atomic Energy and RF President Grants Program (Russia), CAPES, CNPq, FAPERJ, FAPESP and FUNDUNESP (Brazil), Departments of Atomic Energy and Science and Technology (India), Colciencias (Colombia), CONACyT (Mexico), KRF (Korea), CONICET and UBACyT (Argentina), The Foundation for Fundamental Research on Matter (The Netherlands), PPARC (United Kingdom), Ministry of Education (Czech Republic), Natural Sciences and Engineering Research Council and WestGrid Project (Canada), BMBF (Germany), A.P. Sloan Foundation, Civilian Research and Development Foundation, Research Corporation, Texas Advanced Research Program, and the Alexander von Humboldt Foundation.

[1] The DØ Collaboration, S.Abachi *et al.*, "The DØ Upgrade: The Detector and its Physics", Fermilab Pub-96/357-E (1996).
[2] J. M. Campbell, R. K. Ellis, Phys. Rev. **D 60** 113006, hep-ph/9905386 (1999).
[3] F. Abe *et. al*, The CDF Collaboration, Phys. Rev. Lett. 78, 4537 (1997).
[4] T. Sjostrand, P. Eden, C. Friberg, L. Lonnblad, G. Miu, S. Mrenna and E. Norrbin, Comput. Phys. Commun. 135 238 (2001), hep-ph/0010017 (2000).
[5] M.L. Mangano, M. Moretti, F. Piccinini, R. Pittau, A. Polosa, JHEP 0307:001 (2003), hep-ph/0206293 (2002).
[6] CTEQ Collab., H. L. Lai et al., Phys. Rev. D **55** 1280 (1997).
[7] R. Hamberg, W. L. van Neerven and T. Matsuura, Nucl. Phys. **B359** 343 (1991) [Erratum-ibid. B 644 403 (2002)].
[8] N. Kidonakis and R. Vogt, Phys. Rev. **D 68** 114014 (2003).
[9] K. Hagiwara et al., Review of Particle Physics, Physical Review D 66, 010001 (2002).
[10] G. J. Feldman and R. D. Cousins, Phys. Rev. D **57** 3873 (1998), physics/9711021 (1997).
[11] B. P. Roe and M. B. Woodroofe, Phys. Rev. D **60** 053009 (1999), physics/9812036 (1998).
[12] T. Junk, Nucl. Instr. and Methods, **A 434** 435 (1999).